Cases of Soft Switching in a Series Resonant Balancing Converter for Bipolar DC Grids

Yadav, Sachin; Qin, Zian; Bauer, Pavol

DOI
10.1109/IECON49645.2022.9969022

Publication date
2022

Document Version
Final published version

Published in
IECON 2022 - 48th Annual Conference of the IEEE Industrial Electronics Society

Cases of Soft Switching in a Series Resonant Balancing Converter for Bipolar DC Grids

Sachin Yadav
DC Energy Conversion and Storage
TU Delft
Delft, The Netherlands
S.Yadav-1@tudelft.nl

Zian Qin
DC Energy Conversion and Storage
TU Delft
Delft, The Netherlands
Z.Qin-2@tudelft.nl

Pavol Bauer
DC Energy Conversion and Storage
TU Delft
Delft, The Netherlands
P.Bauer@tudelft.nl

IECON 2022 – 48th Annual Conference of the IEEE Industrial Electronics Society | 978-1-6654-8025-3/22/$31.00 ©2022 IEEE | DOI: 10.1109/IECON49645.2022.9969022

***Abstract*—Balancing converters are an integral part of a bipolar dc grid. Resonant converter topologies are interesting for power electronics engineers due to their soft switching capabilities. A series resonant converter topology is promising as a balancing converter in a bipolar dc grid. The series resonant converter is usually a non-inverting topology. However, in the balancing converter application, the converter is used as an inverting type, like a buck-boost converter topology. In this paper, the soft switching capabilities of this converter are shown and analyzed for four distinct converter modulation schemes.**

***Index Terms*—balancing converter, bipolar dc, power electronics.**

I. Introduction

The dc grids can be unipolar or bipolar. Bipolar dc grids have several advantages compared to unipolar dc grids [1]. They have improved reliability because of multiple conductors/poles; if one pole is faulty, then the other can be used to supply half of the power. They have increased flexibility because of more than one voltage level. Hence, bipolar dc grids are being considered for future dc grids.

Balancing converters are an integral part of bipolar dc grids. Many topologies exist for these converters in the literature [2]–[8]. One of the ways to form a bipolar dc grid is by using a three-level converter to interface the synchronous generator. Three-phase multilevel converter topologies like Neutral Point Clamped and T-Type converters can achieve the balancing function [2], [3]. These converters are controlled, so the voltage at the dc side remains balanced, and no current flows in the neutral line [9]. However, they can have additional current stresses on the semiconductor switches leading to non-uniform heating. The three-level converters can be used even in case of unbalances on the dc side. However, an unbalanced dc operation leads to increased total harmonic distortion on the ac side, thus leading to higher losses in the machine interfaced with the converter [10]. Also, the dc-link capacitors' size becomes high to attenuate the effect of the unbalances [11]. It is also challenging to have a distributed architecture using these converters.

Other balancing converter topologies include Buck-Boost, Cuk, and SEPIC converters [6], [7]. These inverting topologies can be directly utilized as balancing converters in a bipolar dc grid [4]. Another interesting topology is a series-resonant converter topology. This converter is a type of non-inverting topology. Hence, it can not be used as a balancing converter without some modifications. In this work, we discuss and analyze the soft switching capability of this topology. It will be shown that the converter can function in both the capacitive and inductive regions. Also, soft-switching can be achieved with zero voltage switching (ZVS) in all the switches or a combination of ZVS and zero current switching (ZCS).

The structure of this paper is as follows. The converter operating principle for the various operating modes is discussed in section II. Section III shows and discusses the simulation results of the different operating modes. Finally, the conclusions are given in section IV.

II. Converter operating principle

The converter is based on a series-resonant converter topology, as shown in figure 1. This topology is conventionally used as non-inverting. However, this topology is used as an inverting topology in our application.

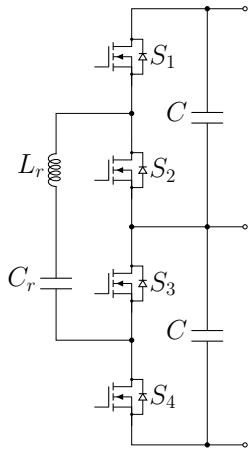

Fig. 1: Balancing converter based on a series resonant converter topology.

A. Phase Shift Control - Capacitive region

In this mode, the converter's switching frequency is lower than the resonant frequency of the series resonant tank (consisting of L_r and C_r). In such a case, the current in the switch

is leading the applied voltage, which cannot lead to ZVS. However, in this modulation, the operation below the resonant frequency and introducing a phase shift between the upper and lower half bridges, ZVS, is made possible. The same is illustrated in figure 2.

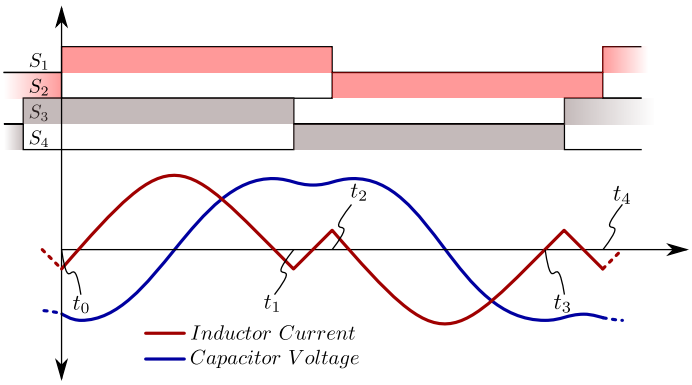

Fig. 2: Converter states in phase shift control - capacitive region.

The operating principle of the converter is given below. The dead time between the switching has been neglected for this analysis. It can be seen from figure 2 that the inductor current is negative before S_3 is turned off and S_4 is turned on. When S_3 is turned off, the current is non-negative and transfers to the body diode of switch S_4. This current discharges the output capacitance Coss of the switch, which leads to the ZVS turn-on. Similarly, the ZVS operation for other switches can also be explained. These are explained for each time interval below.

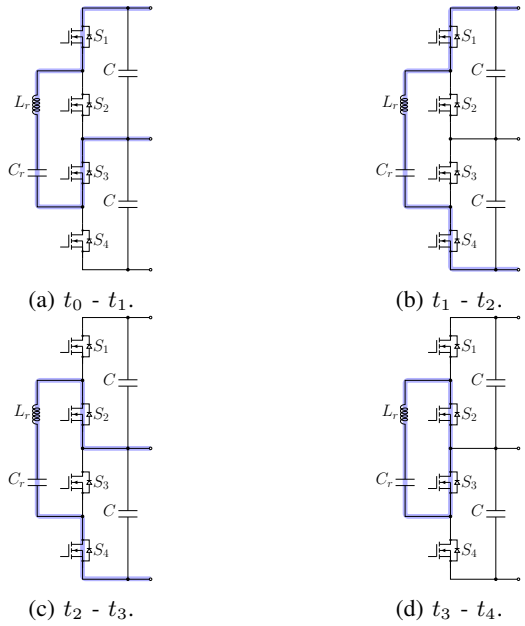

(a) t_0 - t_1. (b) t_1 - t_2. (c) t_2 - t_3. (d) t_3 - t_4.

Fig. 3: Operation of the resonant converter in different periods in case the converter operates in the capacitive region with phase shift control.

- $\mathbf{t_0}$ - $\mathbf{t_1}$: Switches S_1 and S_3 are conducting in this state. S_1 is turned on at t_0 with soft switching. The resonant capacitor C_r charges, and the resonant inductor L_r limit the current. At the end of this interval, the inductor current is negative to discharge the C_{oss} of the semiconductor switch.
- $\mathbf{t_1}$ - $\mathbf{t_2}$: At t_1, switch S_3 is turned off and switch S_4 is turned on at zero voltage. Now, switches S_1 and S_4 are conducting. Hence, there is a higher voltage present across the resonant capacitor C_r. Due to this stage, the charge is pumped into the resonant capacitor. This extra charge stored in the capacitor is used to boost the voltage of the output capacitor and supply the extra energy. Before the end of this interval, the current becomes positive, as shown in figure 2. When S_1 is turned off, this positive current flows through the body diode of S_2. Hence, the C_{oss} of the switch is discharged.
- $\mathbf{t_2}$ - $\mathbf{t_3}$: At t_2, switch S_2 turns on with zero voltage across its drain and source. The resonant tank is connected to the neutral and negative poles through switches S_2 and S_4. After a short moment, the inductor current reverses direction, and the capacitor discharges to transfer the energy to the load. At the end of this interval, the inductor current changes direction and becomes positive. Now, the current flow through the body diode of S_3. Hence, the C_{oss} of S_3 charges before it turns on.
- $\mathbf{t_3}$ - $\mathbf{t_4}$: At t_3, switch S_4 turns off, and S_3 turns on with soft switching. Hence, the resonant tank current freewheels through the switches and inductor reduce to become negative before the end of the interval. As the current negative, it starts flowing through the body diode of S_1. Hence, the C_{oss} of S_1 is discharged, and the switch is ready to be turned on with soft switching.

It should be noted that the stages $\mathbf{t_1}$ - $\mathbf{t_2}$ and $\mathbf{t_3}$ - $\mathbf{t_4}$ can be generated by a phase shift between the upper half-bridge (consisting of switches S_1 & S_2) and the lower half-bridge (consisting of switches S_3 & S_4).

B. Phase Shift Control - Inductive region

In this operating mode, the converter operates above the resonant frequency of the series resonant tank consisting of L_r and C_r. The current lags the switch voltage and leads to the ZVS turn-on of the switches at specific operating points. The converter states consisting of the inductor current and capacitor voltage are shown in figure 4. It should be noted that the starting point of the converter operation is arbitrarily chosen.

The converter operation in the inductive region is detailed below using figures 4 and 5.

- $\mathbf{t_0}$ - $\mathbf{t_1}$: Initially, S_4 is on, and at t_0, S_1 turns on with ZVS. The voltage imposed on the resonant tank is the complete +pole to -pole voltage. Hence, the current rises rapidly. Before the end of this interval, the inductor current is positive. At the end of this interval, S_4 turns off. Hence, the inductor current transfers to the body diode of

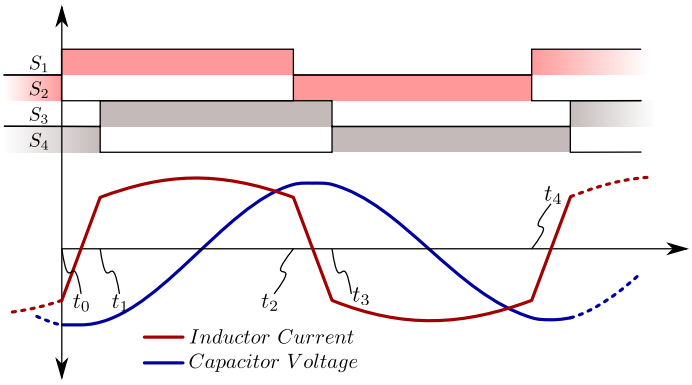

Fig. 4: Converter states in phase shift control - inductive region.

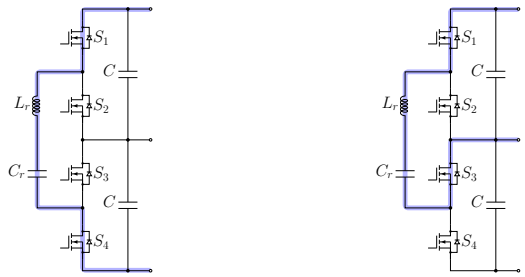

(a) t_0 - t_1. (b) t_1 - t_2.

(c) t_2 - t_3. (d) t_3 - t_4.

Fig. 5: Operation of the resonant converter in different periods in case the converter operates in the inductive region with phase shift control.

S_3. This current discharges the C_{oss} of S_3 and prepares it for ZVS turn-on.

- $\mathbf{t_1}$ - $\mathbf{t_2}$: At t_1, S_3 turns on with ZVS. In this interval, the inductor current stays positive. At the end of this interval, S_1 turns off. The inductor current flows through S_1 and transfers to the body diode of S_2. This current discharges the C_{oss} of S_2 and prepares it for ZVS turn-on.
- $\mathbf{t_2}$ - $\mathbf{t_3}$: At t_2, S_2 turns on with ZVS. During this interval, the resonant tank shorts through switches S_2 and S_3. Hence, the current reduces rapidly and becomes negative. At the end of this interval, S_3 turns off. The negative inductor current now flows through the body diode of S_4. This current discharges the C_{oss} of S_4 and prepares it for ZVS turn-on.
- $\mathbf{t_3}$ - $\mathbf{t_4}$: At t_3, S_4 turns on with ZVS. During this interval, the inductor stays negative and does not change direction. At the end of this interval, S_2 turns off. The inductor current now flows through the body diode of S_1 and discharges its C_{oss} to prepare it for the ZVS turn-on.

C. Duty Cycle Control- Capacitive region

In this mode, take advantage of both ZVS and ZCS for soft switching. In this section, the operation in this mode is discussed.

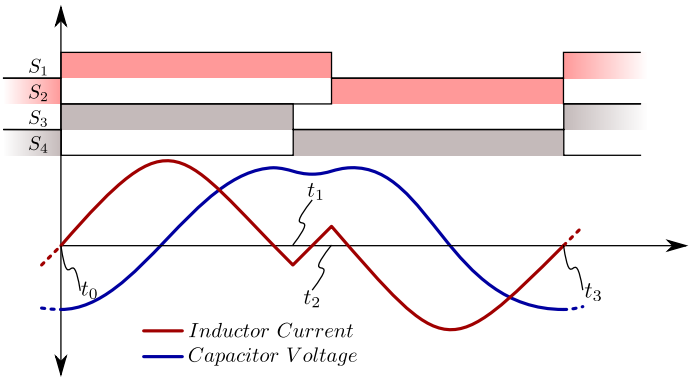

Fig. 6: Converter states in duty cycle control - capacitive region.

The switching states and resonant tank states are shown in figure 6. The states are divided between three time intervals, as illustrated in figure 7. The converter operation is explained below.

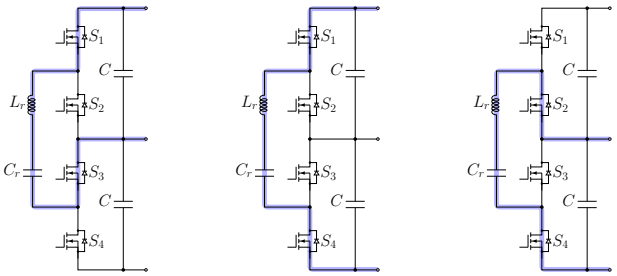

(a) t_0 - t_1. (b) t_1 - t_2. (c) t_2 - t_3.

Fig. 7: Operation of the resonant converter in different periods in case the converter operates in the capacitive region with duty cycle control.

- $\mathbf{t_0}$ - $\mathbf{t_1}$: At t_0, both S_1 and S_3 turn on. The inductor current is almost zero at this instant. Hence, the switches turn on with ZCS. At the end of this interval becomes negative; S_3 turns off, and the inductor current starts flowing through the body diode of S_4, discharging its C_{oss} and making it ready for ZVS turn-on.
- $\mathbf{t_1}$ - $\mathbf{t_2}$: At t_1, S_4 is turned on with ZVS. With S_1 and S_4 on, the voltage across the resonant tank increases. Hence, the current through the resonant inductor increases rapidly. Before the end of this interval, the current becomes positive. At the end of this interval, S_1 turns off.

Hence, the inductor current starts flowing through the body diode of S_2 and prepares it for ZVS turn-on.

- $\mathbf{t_2}$ - $\mathbf{t_3}$: At t_2, S_2 turns on with ZVS. During this interval, the current stays negative for a long time. At the end of this interval, the inductor becomes zero. At that moment, both S_2 and S_4 turn off.

D. Duty Cycle Control - Inductive region

Similar to the capacitive region, this mode exhibits ZVS and ZCS during switching. Figure 8 shows the converter's resonant states and switch states.

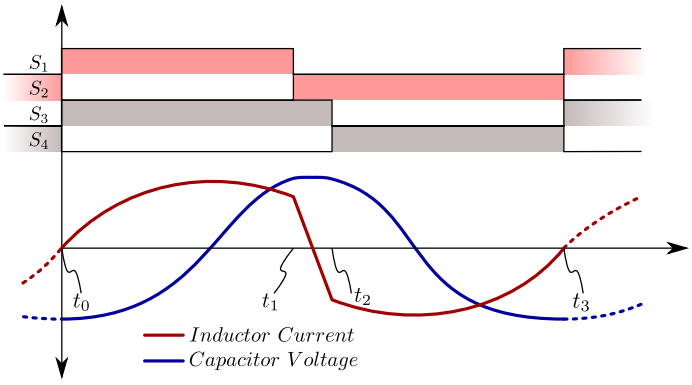

Fig. 8: Converter states in duty cycle control - inductive region.

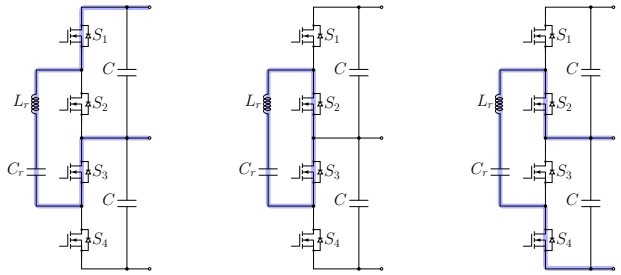

(a) t_0 - t_1. (b) t_1 - t_2. (c) t_2 - t_3.

Fig. 9: Operation of the resonant converter in different periods in case the converter operates in the inductive region with duty cycle control.

- $\mathbf{t_0}$ - $\mathbf{t_1}$: Similar to the first interval of capacitive, in this mode, both S_1 and S_3 turn on with ZCS. The inductor current stays positive during this interval. At the end of this interval, S_1 turns off. The inductor current starts flowing through the body diode of S_2, thus discharging its C_{oss} and preparing it for ZVS turn on.
- $\mathbf{t_1}$ - $\mathbf{t_2}$: This interval is similar to the phase shift control inductive region.
- $\mathbf{t_2}$ - $\mathbf{t_3}$: At t_2, S_4 turns on with ZVS. The current stays negative during this interval. At t_3, the inductor current becomes zero and switches S_2 and S_4 are turned off.

III. Simulation Results

This section shows and discusses the results of the different modes of the balancing converter. The simulations are done in PLECS™ software and the converter parameters are shown in table I.

TABLE I: Specifications of the converter.

Parameter	Value
Grid Voltage	$\pm 350\ V$
Resonant Inductor (L_r)	$7\ \mu H$
Resonant Capacitor (C_r)	$594\ nF$
DC Link Capacitor (C)	$1000\ \mu F$

Some general points are followed for all the operating modes. These are listed as follows.

- Inductor current initial values are fixed at 3A.
- The dead time is ignored for all the switches. However, it will have a significant impact.
- The grid conditions are the same for all the simulations. The load is considered as a constant current of 10A. It is connected between the neutral and negative poles.

The grid and the connection of the converter are shown in figure 10. The source consists of two series-connected voltage source converters with output voltage fixed at 350V. The lumped line elements simulate the resistance, inductance, and capacitance of a certain length of cable. The unbalanced load is represented by a load converter connected only between the neutral and - poles of the grid.

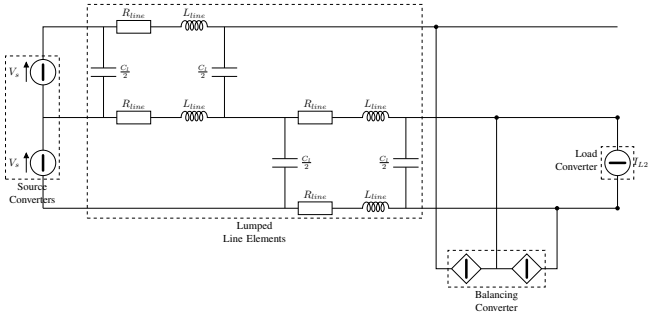

Fig. 10: Schematic of the test setup.

The simulation results when the unbalanced load current is 10A are shown and discussed below. In each result plot, a subplot of V_{pn} and V_{nm} shows the balanced voltages due to the balancing converter.

A. Phase Shift Control - Capacitive region

The results of the simulation of the balancing converter operating in the capacitive region with phase shift control are shown in figure 11. For balancing the voltage, the converter is operated at 69118 Hz. The lower half bridge leads the upper half bridge by 3.6 deg. For an output current of 10A, this mode has the highest peak inductor current compared to the other power modes. Also, the change in the capacitor voltage is the highest.

B. Duty Cycle Control - Capacitive region

The results for the simulation of the balancing converter operating in the capacitive region with duty cycle control are

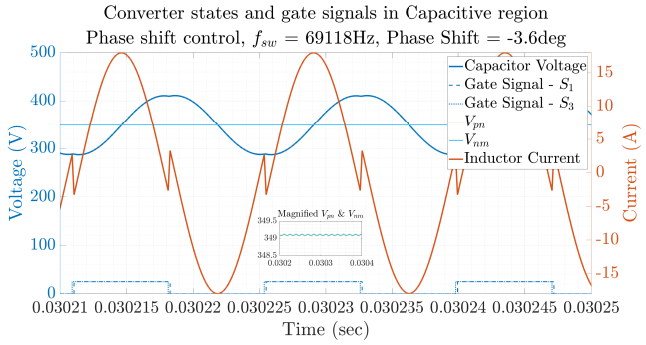

Fig. 11: Results of PLECS simulation for Phase Shift control - Capacitive region.

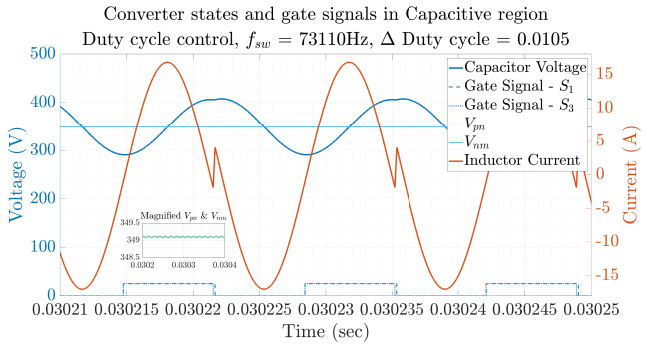

Fig. 12: Results of PLECS simulation for Duty Cycle control - Capacitive region.

shown in figure 12. The converter is operating at 73110 Hz. S_1 and S_2 have a duty cycle of 50%. However, the duty cycle of S_3 is (50-1.05)%, and that of S_4 is (50+1.05)%. Hence, the difference in the duty cycle of the lower bridge with the upper bridge is 1.05%. This duty cycle is denoted by Δ Duty cycle. During this interval, the inductor current increases as there is a higher voltage across the resonant when S_1 and S_4 are conducting. In this mode, the peak inductor current and capacitor voltage change are lower than in the phase shift control mode.

C. Phase Shift Control - Inductive region

The results of the simulation of the balancing converter operating in the inductive region with phase shift control are shown in figure 13. The converter needs to operate above the resonant frequency at 88497 Hz. For the given direction of power flow, the lower half bridge is lagging the upper one by 3.37 deg. In this mode, the peak inductor current and capacitor voltage change are further reduced.

D. Duty Cycle Control - Inductive region

The results of the simulation of the balancing converter operating in the inductive region with duty cycle control are shown in figure 14. The converter needs to operate at 82670 Hz with a Δ Duty cycle of 0.87%.

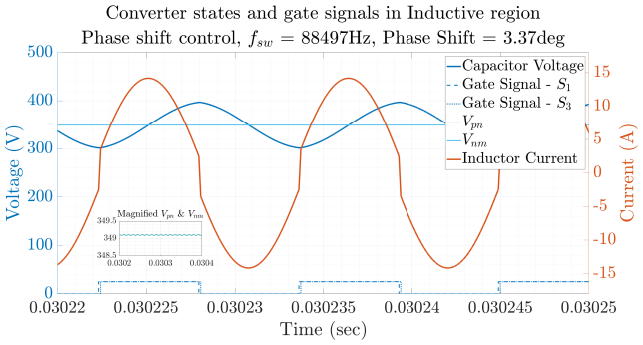

Fig. 13: Results of PLECS simulation for Phase Shift control - Inductive region.

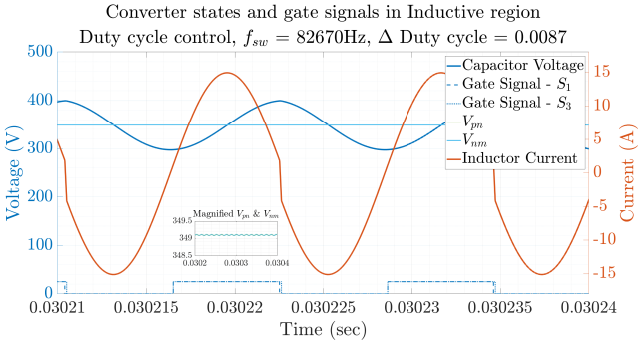

Fig. 14: Results of PLECS simulation for Duty Cycle control - Inductive region.

E. Power flow characteristics

The power flow from one pole to the other depends upon the switching frequency and phase shift/duty cycle between/of the upper and lower half bridge legs. The relationship between the two modes in the capacitive region is shown in figure 15. These relationships are plotted for ZVS & ZCS conditions and when the current at the different switching instances is approximately +/-3A.

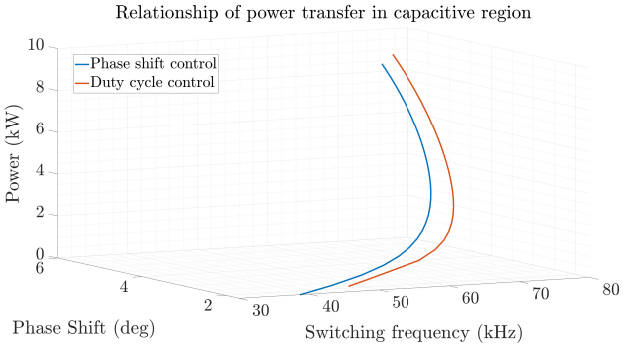

Fig. 15: Power flow characteristics - capacitive region.

Similarly, the power transfer relationship with switching frequency and phase shift/duty cycle is shown in figure 16. It can be seen that the change of power delivered with respect to the switching frequency and phase shift is more steep

compared to the case of capacitive region operation. Hence, controlling the power flow can be more difficult in this region.

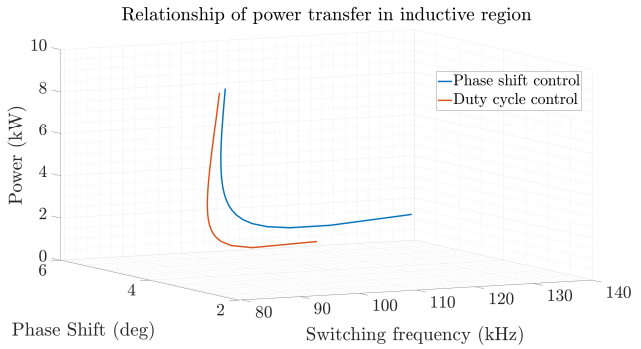

Fig. 16: Power flow characteristics - inductive region.

IV. Conclusion

This paper shows the soft switching capabilities of a series resonant balancing converter for the application of balancing a bipolar dc grid. The converter can operate in four distinct modes. Firstly, the converter can operate in the capacitive or inductive region. This choice has an impact on the selection of passive components. Generally speaking, the passive components' size decreases as the converter's designed switching frequency increases. Hence, the designer might design the converter to operate in the inductive region. However, this increases the complications because the rated RMS voltage for the capacitor decreases with the switching frequency. Hence, resonant capacitors' failure probability increases in the inductive region – also, the losses in the inductor increase with frequency.

Additionally, the maximum flux density for the ferrite core materials suitable for higher than 100 kHz is limited (50-100 mT) [12]. The peak allowed flux density is vital as the current through the inductor is almost sinusoidal. Hence, the peak flux in the worst case needs to be lower than the maximum allowed of 50-100 mT. Additionally, the converter control also becomes more complicated in the inductive region, as discussed in the previous section with the help of figure 16.

Secondly, the converter can be operated by changing the phase shift between the upper and lower half bridges or the duty cycle of one half-bridge while keeping it fixed at 50% for the other half-bridge. The choice of half-bridge for the duty cycle change depends upon the power flow direction (from +ve pole to -ve pole and vice versa) and the operating region (inductive or capacitive). Theoretically, all operating conditions can achieve ZVS for phase shift control. On the other hand, for the duty cycle control ZVS turn on is achieved for two switches at the switching instances t_2 and $t3$ whereas ZCS is achieved for all switches at t_0 and t_3. Hence, the switches losses in the duty cycle control can be slightly higher. Another aspect to consider is that the phase shift and duty cycle would decrease when the switching frequency increase for the same current value at switching instants. The previous statement implies that the control becomes more difficult with increasing power output for the capacitive region as the power output increases with increasing frequency. On the other hand, the control becomes easier for the inductive region because the power output increases with decreasing frequency.

This analysis neglects the dead time. However, it is an essential parameter for the successful operation of this converter. It should be sufficiently high to discharge the C_{oss} with the amount of current at the switching instant and should be sufficiently small to not let the inductor current freewheel in resonance with the C_{oss} of switches and change direction before the next switching instant. A detailed analysis of dead time is beyond the scope of this paper.

References

[1] B. S. H. Chew, Y. Xu, and Q. Wu, "Voltage Balancing for Bipolar DC Distribution Grids: A Power Flow Based Binary Integer Multi-Objective Optimization Approach," *IEEE Transactions on Power Systems*, vol. 34, no. 1, pp. 28–39, Jan. 2019.

[2] J. Lago, J. Moia, and M. L. Heldwein, "Evaluation of power converters to implement bipolar DC active distribution networks — DC-DC converters," in *2011 IEEE Energy Conversion Congress and Exposition*. Phoenix, AZ, USA: IEEE, Sep. 2011, pp. 985–990.

[3] J. Moia, J. Lago, A. J. Perin, and M. L. Heldwein, "Comparison of three-phase PWM rectifiers to interface Ac grids and bipolar Dc active distribution networks," in *2012 3rd IEEE International Symposium on Power Electronics for Distributed Generation Systems (PEDG)*. Aalborg: IEEE, Jun. 2012, pp. 221–228.

[4] F. Wang, Z. Lei, X. Xu, and X. Shu, "Topology Deduction and Analysis of Voltage Balancers for DC Microgrid," *IEEE Journal of Emerging and Selected Topics in Power Electronics*, vol. 5, no. 2, pp. 672–680, Jun. 2017.

[5] G. Van den Broeck, J. Beerten, M. Dalla Vecchia, S. Ravyts, and J. Driesen, "Operation of the full-bridge three-level DC–DC converter in unbalanced bipolar DC microgrids," *IET Power Electronics*, vol. 12, no. 9, pp. 2256–2265, Aug. 2019.

[6] P. Najafi, A. Houshmand Viki, and M. Shahparasti, "Evaluation of Feasible Interlinking Converters in a Bipolar Hybrid Microgrid," *Journal of Modern Power Systems and Clean Energy*, vol. 8, no. 2, pp. 305–314, 2020.

[7] S. Rivera, R. Lizana F., S. Kouro, T. Dragicevic, and B. Wu, "Bipolar DC Power Conversion: State-of-the-Art and Emerging Technologies," *IEEE Journal of Emerging and Selected Topics in Power Electronics*, vol. 9, no. 2, pp. 1192–1204, Apr. 2021.

[8] S. Yadav, Z. Qin, and P. Bauer, "Bipolar DC grids on ships: Possibilities and challenges," *e & i Elektrotechnik und Informationstechnik*, Jun. 2022.

[9] S. Rivera, B. Wu, S. Kouro, V. Yaramasu, and J. Wang, "Electric Vehicle Charging Station Using a Neutral Point Clamped Converter With Bipolar DC Bus," *IEEE Transactions on Industrial Electronics*, vol. 62, no. 4, pp. 1999–2009, Apr. 2015.

[10] B. Wu and M. Narimani, *High-power converters and AC drives*. John Wiley & Sons, 2017.

[11] J. Pou, R. Pindado, D. Boroyevich, and P. Rodríguez, "Evaluation of the low-frequency neutral-point voltage oscillations in the three-level inverter," *IEEE transactions on industrial electronics*, vol. 52, no. 6, pp. 1582–1588, 2005.

[12] Ferroxcube. Soft ferrites and accessories. [Online]. Available: https://www.ferroxcube.com/en-global/download/download/11